Proc. Natl. Acad. Sci. USA
Vol. 88, pp. 3525–3529, May 1991
Cell Biology

Functional analysis of human cardiac gap junction channel mutants

(single channels/heart/electrophysiology/SKHep1 cells/connexin)

GLENN I. FISHMAN*†, ALONSO P. MORENO‡, DAVID C. SPRAY‡, AND LESLIE A. LEINWAND§

*Department of Medicine, Division of Cardiology, ‡Department of Neuroscience, and §Department of Microbiology and Immunology, Albert Einstein College of Medicine, 1300 Morris Park Avenue, Bronx, NY 10461

Communicated by Dominick P. Purpura, January 11, 1991 (received for review November 8, 1990)

ABSTRACT **The connexins form a family of membrane spanning proteins that assemble into gap junction channels. The biophysical properties of these channels are dependent upon the constituent connexin isoform. To begin identifying the molecular basis for gap junction channel behavior in the human heart, a tissue that expresses connexin43, we used site-directed mutagenesis to generate mutant cDNAs of human connexin43 with shortened cytoplasmic tail domains. Premature stop codons were inserted, resulting in proteins corresponding in length to the mammalian isoforms connexin32 and connexin26, which are expressed primarily in liver. All constructs restore intercellular coupling when they are transfected into SKHep1 cells, a human hepatoma line that is communication deficient. Whereas wild-type connexin43 transfectants display two distinct unitary conductance values of about 60 and 100 pS, transfectants expressing the mutant proteins, from which 80 and 138 amino acids have been deleted, exhibit markedly different single-channel properties, with unitary conductance values of about 160 and 50 pS, respectively. Junctional conductance of channels composed of wild-type connexin43 is less voltage-sensitive compared with transfectants expressing wild-type connexin32. However, neither of the connexin43 truncation mutants alters this relative voltage insensitivity. These results suggest that the cytoplasmic tail domain is an important determinant of the unitary conductance event of gap junction channels but not their voltage dependence. Furthermore, since the mutant connexins are missing several consensus phosphorylation sites, modification of these particular sites may not be required for membrane insertion or assembly of human connexin43 into functional channels.**

Gap junctions are specialized regions of adjoining cell membranes typically composed of numerous intercellular low resistance channels. Each channel is thought to consist of 12 connexin monomers, which assemble as coaxially aligned pairs of hexameric hemichannels. By permitting the passage of ions and chemical mediators from cell to cell, gap junction channels are likely to play a major role in a wide variety of cellular processes, including embryogenesis, cellular differentiation and development, and electrotonic coupling (for reviews see refs. 1 and 2). The connexins constitute a family of proteins whose expression is tissue specific and developmentally regulated (3–7). This diversity presumably reflects the temporal and/or spatial requirement of different tissues for the unique biophysical properties associated with channels assembled from particular connexin isoforms. These properties include the unitary conductance value, as well as channel gating characteristics in response to transjunctional potential, intracellular pH or Ca^{2+} concentration, and second messenger molecules.

There is considerable speculation about the structural domains of connexins that determine their unique functional characteristics (8). Theoretical modeling based on sequence analysis, as well as comparison to other classes of proteins, such as those that form the ion-specific channels, suggest possible molecular mechanisms that confer specific channel properties. We have previously described the use of stable transfection of a communication-deficient human hepatoma cell line (SKHep1) to determine the biophysical properties of channels composed of exogenous connexins (9, 10). Transfection of the cDNA encoding human connexin43 protein resulted in clones that became functionally coupled, as evaluated by both the intercellular diffusion of Lucifer yellow and direct electrophysiological measurements. Single-channel recordings revealed a unitary conductance value for channels formed by the human connexin43 protein that were similar to those previously reported for cardiocytes from other mammals (9).

Here we describe the further analysis of cell lines that express wild-type human connexin43, as well as carboxy-terminal truncation mutants of connexin43 that correspond in length to the cytoplasmic tails found in two other mammalian gap junction proteins, connexin32 and connexin26. Intercellular coupling is restored in cell lines expressing either of these truncation mutants; however, the unitary conductance values differ from those channels formed from full-length human connexin43. No appreciable difference in transjunctional voltage sensitivity is apparent among the three cell lines. These results suggest that the cytoplasmic tail domain is an important determinant of the unitary conductance event, but it does not influence transjunctional voltage sensitivity and is not necessary for assembly of human connexin43 into functional channels.

METHODS

Site-Directed Mutagenesis. Isolation and characterization of clones representing a full-length human cardiac gap junction (HCGJ, human connexin43) cDNA have been described previously (9). Site-directed mutagenesis was performed by using a modification of the protocol of Kunkel (11). Specific mutagenic oligonucleotides were designed to result in premature stop codons, replacing either the aspartic residue at position 245 or the lysine residue at position 303. To facilitate identification of clones harboring mutants, new restriction enzyme sites were also encoded by the oligonucleotides. Mutations were then confirmed by dideoxy sequencing.

Construction of Eukaryotic Expression Plasmids. All plasmids were derived from the Rous sarcoma virus (RSV) expression vector pRSVCAT (26). The wild-type human connexin43 expression plasmid pGF1 has been described previously (9). Plasmids pGF4 and pGF5 were created by replacing a fragment of pGF1 with the corresponding mutated fragments that contained the premature stop codons.

The publication costs of this article were defrayed in part by page charge payment. This article must therefore be hereby marked "*advertisement*" in accordance with 18 U.S.C. §1734 solely to indicate this fact.

Abbreviations: HCGJ, human cardiac gap junction; RSV, Rous sarcoma virus; LTR, long terminal repeat.

†To whom reprint requests should be addressed.

Cell Culture and DNA Transfections. SKHep1 cells were maintained in Dulbecco's modified Eagle's medium (DMEM) supplemented with 10% fetal bovine serum (HyClone), penicillin at 50 international units/ml, streptomycin at 50 μg/ml, and 2 mM L-glutamine. Cells were cotransfected with the pGF expression vector (25 μg) and the dominant selectable marker pSV7Neo (2.5 μg), using a modification of the calcium phosphate coprecipitation technique (12–14). Selection was begun 24 hr after transfection with the addition of G418 (Geneticin, GIBCO) to the medium at 400 μg/ml, and individual colonies were picked by using cloning rings and subsequently analyzed.

Electrophysiology. Clones were screened for the presence of gap junction channels by the ability to transfer Lucifer yellow dye; positive clones were then further analyzed for electrical coupling, as previously described (9). Briefly, cells were plated onto 1-cm coverslips and experiments were performed at room temperature while continuously exchanging the bath solution (160 mM NaCl/7 mM CsCl/0.1 mM $CaCl_2$/0.6 mM $MgCl_2$/1.0 mM Hepes, pH 7.2). Each cell of a pair was voltage clamped at −40 mV by using heat-polished patch pipettes filled with a solution at pCa 8 (135 mM CsCl/0.5 mM $CaCl_2$/2 mM $MgCl_2$/5.5 mM EGTA/5 mM Hepes–KOH, pH 7.2). Cell pairs were uncoupled by the addition of halothane (1.5–2.0 mM) to the bathing solution (15). Under conditions of reduced junctional conductance, single-channel currents were recorded at high gain while imposing a constant transjunctional driving force of 20–50 mV. Currents and voltages were continuously monitored on a four-channel chart recorder (Gould, Cleveland, OH) and recorded on videotape after digitization (Neurocorder, New York).

RESULTS

Eukaryotic Expression Plasmids Are Integrated into the Genome. For each construct (pGF1, pGF4, and pGF5), one or more independent clonal lines were selected on the basis of transfer of Lucifer yellow dye and then expanded for further study. Chromosomal integration of the expression plasmid was confirmed for clonal lines containing each of the three constructs (pGF1, pGF4, and pGF5) by genomic blot hybridization, as shown in Fig. 1. Genomic DNA prepared from either human fetal brain or nontransfected SKHep1 cells shows two bands in both the *Eco*RI lane and *Bam*HI lane, corresponding to the true human connexin43 gene and a processed pseudogene (9). Genomic DNA prepared from a pGF1 transfectant (pGF1-1) shows new bands of the predicted size whose intensity would result from integration of ≈10 copies of the expression plasmid. A similar copy number is seen in a clone harboring pGF4 (pGF4-10), whereas a pGF5 clone (pGF5-8) contains a single copy. Clone pGF4-4, which was G418 resistant, did not demonstrate dye transfer or electrical coupling and did not integrate the expression plasmid.

Transcription Is Driven by the RSV Long Terminal Repeat (LTR). Expression of all three pGF cDNAs is directed by the RSV LTR, with termination, splicing, and polyadenylylation supplied by the 3′ simian virus 40 signals (16). Because the connexin43 coding region but not the entire 3′ untranslated region is included in these expression plasmids, fully processed transcripts are significantly shorter (2.7 kb) than the endogenous (3.1 kb) connexin43 mRNA. Northern blot analysis has been used previously to demonstrate this distinction in size, as well as to document the absence of connexin43 mRNA in nontransfected SKHep1 cells (9). To increase our sensitivity and further rule out the possibility of endogenous expression of connexin43 mRNA in nontransfected SKHep1 cells, S1 nuclease studies were carried out (17). An end-labeled single-stranded probe was prepared that includes portions of the RSV LTR and the human connexin43 cDNA.

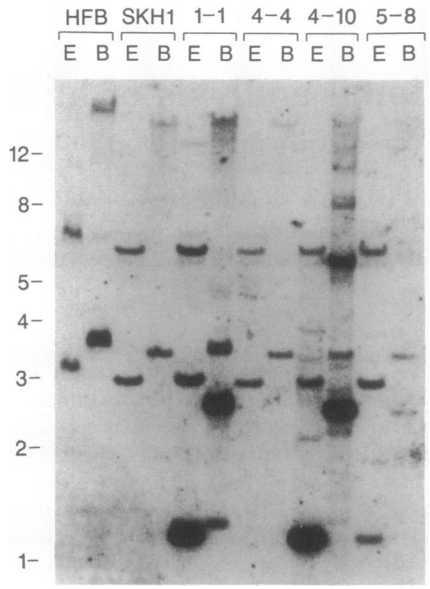

FIG. 1. Chromosomal integration of the pGF expression vectors. Genomic DNA was digested with either *Eco*RI (E) or *Bam*HI (B), electrophoresed on a 1% agarose-TAE gel, transferred to a nylon membrane, and hybridized with a cDNA probe encompassing most of the HCGJ coding region. Hybridization conditions are as previously described (8). Samples included human fetal brain, nontransfected SKHep1 cells (SKH1), pGF1-1 (1-1), pGF4-4 (4-4), pGF4-10 (4-10), and pGF5-8 (5-8). The two bands found in both human fetal brain and nontransfected SKHep1 cells represent the human connexin43 gene and a processed pseudogene. The new bands seen in transfectants pGF1-1, pGF4-10, and pGF5-8 result from integration of the respective expression plasmids. Clone pGF4-4, which was G418 resistant, did not integrate the expression plasmid and was not electrically coupled. Sizes in kilobases (kb) are given on the left.

The strategy for distinguishing between mRNA transcribed from the expression plasmid and from endogenous connexin43 mRNA is shown in Fig. 2*A*. mRNA that is transcribed from pGF plasmids protects a 187-nucleotide fragment, beginning with the RSV transcription initiation site. Human connexin43 mRNA, however, will protect only the 120 nucleotides that are derived from the endogenous transcript. The results of such an assay are shown in Fig. 2*B*. No protected fragments are seen with yeast tRNA (lane 6) or RNA prepared from nontransfected SKHep1 cells (lane 7), consistent with the absence of connexin43-containing gap junction channels in this cell line. Human fetal cardiac RNA (lane 8) protects a 120-nucleotide fragment. RNA from several cell lines carrying pGF expression vectors (lanes 9 and 12) protect a 187-nucleotide fragment. Two transfectants that were G418 resistant but uncoupled do not protect any fragment (lanes 10 and 11), consistent with integration of the neomycin-resistance gene, but not the pGF expression plasmid. No signal that would result from expression of the endogenous human connexin43 gene is seen in any of the transfectants.

Transfectants Are Electrotonically Coupled. Direct confirmation of channel assembly and function was demonstrated by both dye transfer and electrophysiological techniques. Lucifer yellow dye transfer was totally absent in nontransfected SKHep1 cells, but injection of dye into transfectants harboring pGF1 led to its rapid transfer (9). Similar strong coupling was obtained with both pGF4 and pGF5 transfectants (data not shown). To determine the conductance properties of clones expressing each of the three constructs, whole-cell voltage-clamp recordings were obtained from cell pairs. Nontransfected SKHep1 cells typically display low junctional conductance, often below the level of sensitivity

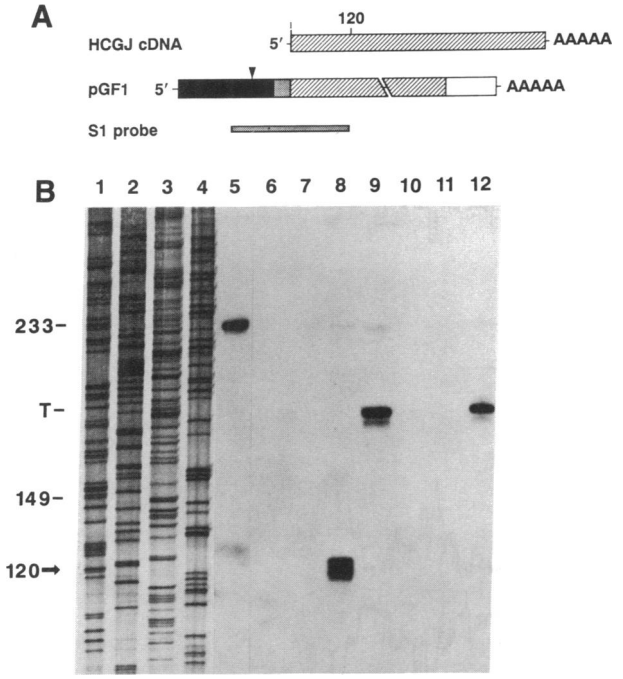

FIG. 2. S1 nuclease protection assay. (*A*) The relationship of the human connexin43 mRNA and a pGF transcript is indicated. Sequences are derived from the RSV LTR (black), polylinker (stippled), human connexin43 cDNA (hatched), and a simian virus 40 fragment that contains the small tumor antigen intron and poly(A) addition site (white). The S1 probe includes 84 nucleotides from the RSV LTR, 29 nucleotides from polylinker sequence, and 120 nucleotides from the human connexin43 (HCGJ) cDNA. The RSV LTR transcription initiation site is indicated by the arrow. Transcription arising from the expression plasmids protects a 187-nucleotide fragment, whereas transcription from the endogenous gene protects only 120 nucleotides. (*B*) S1 analysis of human cardiac and pGF transfectant RNA. Lanes 1–4 include a sequencing reaction of pGF1 generated with the same primer used to prepare the S1 probe. The junction between the human connexin43 cDNA and polylinker is indicated by the arrow. The transcription initiation site is indicated as T. Samples include untreated full-length probe (lane 5), yeast tRNA (lane 6), SKHep1 cells (lane 7), human cardiac RNA (lane 8), pGF1-1 (lane 9), pGF4-1 (lane 10), pGF4-3 (lane 11), and pGF4-10 (lane 12). Transcription from the endogenous gene is seen only with human cardiac RNA. Transcription from the RSV LTR is seen in transfectants pGF1-1 and pGF4-10. No protected fragment is found in nontransfected SKHep1 cells. The probe was hybridized at 30°C for 15 hr with between 5 and 20 μg of total RNA in a buffer consisting of 80% (vol/vol) formamide, 40 mM Pipes at pH 6.4, 50 mM NaCl, and 1 mM EDTA at pH 8.0, at 30°C for 15 hr. The following morning 100 units of S1 nuclease (Boehringer Mannheim) was added, and the mixture was incubated for an additional hour at 30°C. Samples were analyzed on a 4.5% polyacrylamide/6 M urea gel. Approximately 5–20 μg of total RNA was loaded for each sample.

(<20 pS). Expression of each of the constructs increased the junctional conductance markedly, to values typically between 1 and 20 nS (data not shown). Furthermore, cell coupling is rapidly and reversibly disrupted by halothane, a typical feature of cardiac and other gap junction channels (15). After halothane treatment, unitary conductance events were obtained for cell lines expressing the full-length connexin43 protein, as well as for each of the truncation mutants, as shown in Fig. 3. Two discrete values are seen in pGF1 transfectants, corresponding to ≈60 pS and ≈100 pS. Expression of the pGF5 mutation, resulting in truncation of the human connexin43 protein at residue 303, significantly increased the unitary conductance value, averaging ≈160 pS. This channel also appeared less stable, with more flicker between open and closed states. The pGF4 mutation, which truncated the protein at residue 245, had an opposite effect on unitary conductance, decreasing the measured value to ≈50 pS.

The Cytoplasmic Tail Domain Does Not Influence Transjunctional Voltage Sensitivity. The transjunctional voltage sensitivity of transfectants expressing full-length connexin43 as well as the two carboxyl-terminal truncation mutants was also determined. As shown in Fig. 4, channels composed of the wild-type connexin43 were relatively voltage insensitive, with g_{min}, the normalized minimal conductance, ≈0.4 and V_o, the voltage at which g_j is reduced by 50%, > 50 mV. Despite progressive deletion of the cytoplasmic tail, the transjunctional voltage sensitivity of the resulting channels was not appreciably altered.

DISCUSSION

This paper describes the use of eukaryotic transfection and site-directed mutagenesis to begin structure/function analysis of the HCGJ channel. Previously, we reported that channels formed from human connexin43 expressed exogenously in a communication-deficient cell line demonstrated unitary conductance properties typical for channels composed of connexin43 monomers (9). Thus, despite expression within the cellular environment of a hepatoma, these cells exhibited a "cardiac" phenotype with respect to cellular coupling. This included a unitary conductance value of ≈60 pS, which we now show to be only weakly voltage dependent. Interestingly, additional recordings of SKHep1 cells transfected with pGF1 also demonstrate a channel size of ≈100 pS. Although not initially recognized, this observation of two channel sizes represents the first (to our knowledge) demonstration that expression of a single gap junction protein can result in two stable conductance levels. In light of recent studies which demonstrate that connexin43 is a phosphoprotein (18, 19), it should be informative to investigate the possible role of phosphorylation in modulating the equilibrium between these two unitary conductances.

The intracellular domains of the various connexin isoforms, particularly the cytoplasmic loop or hinge region and the cytoplasmic tail, are the most divergent regions of this family of proteins. It has been suggested that these differences in sequence may account for individual channel properties, such as unitary conductance values and gating behavior (8). We therefore began our structure/function analysis by modifying the single most divergent region, the cytoplasmic tail. The truncation mutants presented here were designed to resemble in length, but not in sequence, the cytoplasmic tails found in either connexin32 or connexin26. The conductance properties of channels formed from either of these two truncation mutants differ significantly. Channels composed of pGF5 have a measured unitary conductance value of ≈160 pS. This is of interest because the length of the pGF5 cytoplasmic tail domain approximates that of the wild-type connexin32 protein, whose channels have a similar unitary conductance, as determined in several cell types and expression systems, including acinar cells (20), isolated liver junctional membranes incorporated into lipid bilayers (21, 22), and SKHep1 cells transfected with connexin32 cDNA (10). This result suggests that the cytoplasmic tail plays an important role in determining the unitary conductance event. Measurements of the unitary conductance value for channels containing exclusively connexin26 have not yet been reported, reflecting the inability to identify a tissue that expresses predominantly this isoform. Channels composed of pGF4 have a unitary conductance value of ≈50 pS. It will therefore be of considerable interest to compare the unitary conductance of pGF4 mutant channels with that recorded from SKHep1 cells transfected with the wild-type connexin26 gene. Since the mutations we have analyzed do not

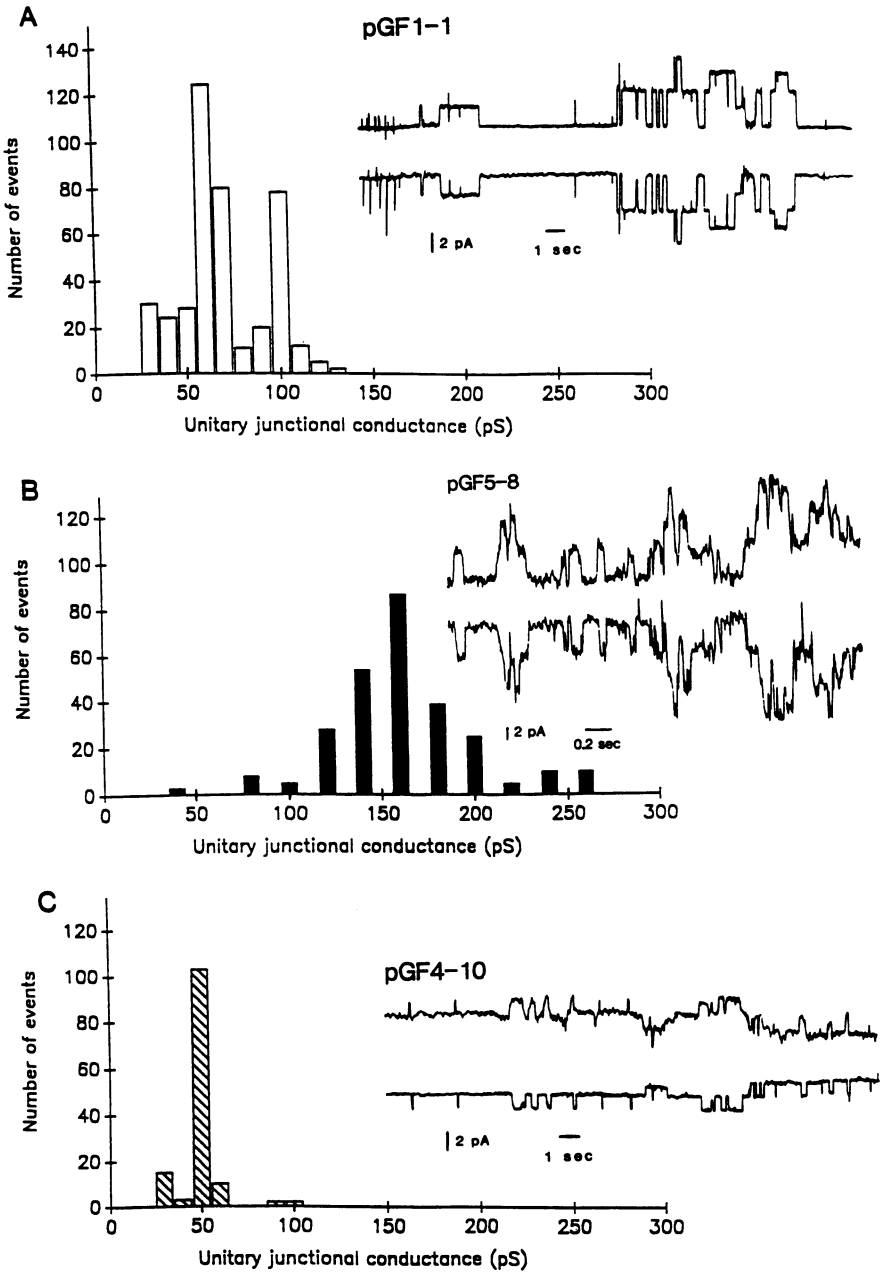

FIG. 3. Unitary conductance events of wild-type and mutant channels. Each cell of a pair was voltage clamped and coupling between cell pairs was reduced by exposure to halothane. Under conditions of reduced junctional conductance, discrete events were detectable; simultaneous divergence of the two cells' currents were indicative of opening of gap junction channels. Histograms of event numbers versus channel size were generated for each transfectant, and the dominant unitary conductance value(s) was determined by curve fitting, assuming a gaussian distribution (Gauss–Newton Software, Assist Software Technologies, Rochester, NY). The pGF1-1 transfectants displayed two major unitary conductance values, 62.6 ± 7.4 pS and 98.9 ± 5.5 pS (*A*; eight cell pairs, 382 events). pGF5-8 transfectants had a unitary conductance value of 157.2 ± 25 pS (*B*; two cell pairs, 178 events), whereas pGF4-10 cell pairs displayed a value of 50.8 ± 4.1 pS (*C*; two cell pairs, 132 events). A minor peak of ≈30 pS is also visible for pGF1-1 and pGF4-10, corresponding to the SKHep1 endogenous channel. Values represent means ± SD for the fitted curves. Representative recordings at transjunctional drive force of 40 mV are shown for each cell line (*Insets*); records were filtered at 30 Hz.

directly affect the presumptive channel-forming region—i.e., the amphipathic third membrane-spanning domain—it appears that conformational changes related to the length of the cytoplasmic tail can significantly alter the rate of ion permeation through the channel pore.

While the unitary conductance event is markedly influenced by the size of the cytoplasmic tail, the transjunctional voltage–conductance relationship appears unaltered by truncation of this domain. Inasmuch as no homologue to the S4 voltage-sensing domain (23) of the sodium channel is found in any of the connexin proteins, the basis for and variation in transjunctional voltage sensitivity of different gap junction channels remain speculative. Our results, however, suggest that the cytoplasmic tail is not involved in modulating the gating response to transjunctional potential.

The system described in this report, exogenous expression of site-directed mutants, has been used to dissect the structure–function relationship of numerous families of proteins, including the β-adrenergic receptor (24) and various ion-selective channels (23, 25). By transfecting mutant cDNA constructs into a communication-deficient cell line, we have now extended this kind of analysis to the connexin family of proteins. Our hope is to characterize the precise features of these and other channel-forming proteins that determine their

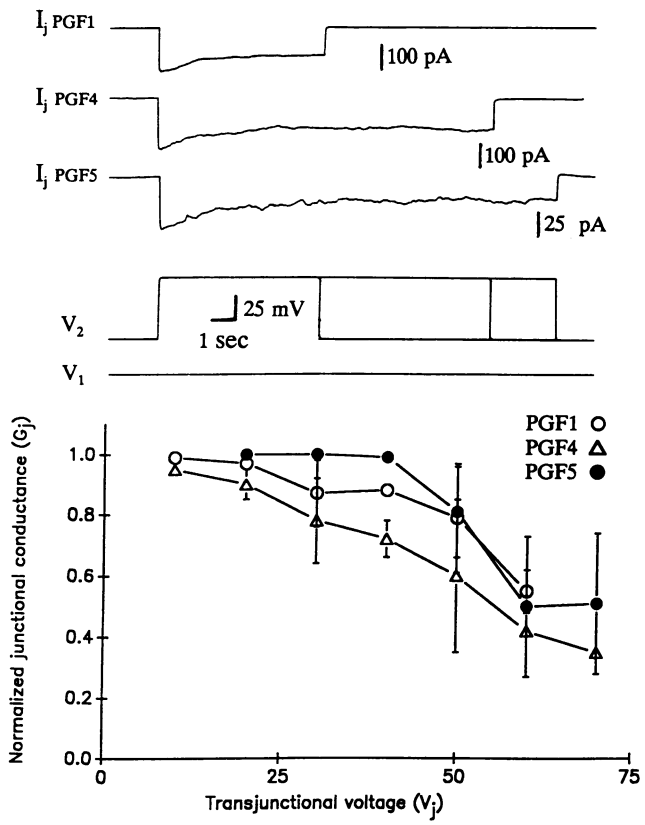

FIG. 4. Voltage dependence of transfectants. (*Upper*) Junctional currents (I_j) recorded in pGF1, pGF4, and pGF5 in response to transjunctional voltages (V_2) of 60 mV. Note similarity in kinetics of relaxation during the voltage step. (*Lower*) Steady-state junctional conductance (normalized) as a function of transjunctional voltage (in mV) for wild-type human connexin43 (pGF1-1) and the two truncation mutants. Values represent means ± SD for at least five experiments in each case.

unique functional properties, such as the unitary conductance event, gating behavior, and ion selectivity. In so doing, the molecular determinants of channel biophysics should become better understood.

G.I.F. is the recipient of National Institutes of Health Physician–Scientist Award 1K11HL02391. G.I.F. and D.C.S. are recipients of grants-in-aid from the American Heart Association, New York City Affiliate. L.A.L. is the recipient of a grant-in-aid from the American Heart Association. This work was supported in part by National Institutes of Health Grants NS16542 and HL38449 to D.C.S. and HL37412 to L.A.L.

1. Bennett, M. V. L. & Spray, D. C., eds. (1985) *Gap Junctions* (Cold Spring Harbor Lab., Cold Spring Harbor, NY).
2. Hertzberg, E. L. & Johnson, R. G., eds. (1988) *Gap Junctions* (Liss, New York).
3. Beyer, E. C., Paul, D. L. & Goodenough, D. A. (1990) *J. Membr. Biol.* **116**, 187–194.
4. Fishman, G. I., Hertzberg, E. L., Spray, D. C. & Leinwand, L. A. (1991) *Circ. Res.* **68**, 782–787.
5. Dermietzel, R., Traub, O., Hwang, T. K., Beyer, E., Bennett, M. V. L., Spray, D. C. & Willecke, K. (1989) *Proc. Natl. Acad. Sci. USA* **86**, 10148–10152.
6. Gimlich, R. L., Kumar, N. M. & Gilula, N. B. (1988) *J. Cell Biol.* **107**, 1065–1073.
7. Gimlich, R. L., Kumar, N. M. & Gilula, N. B. (1990) *J. Cell Biol.* **110**, 597–605.
8. Spray, D. C. & Burt, M. M. (1990) *Am. J. Physiol.* **258**, C195–C205.
9. Fishman, G. I., Spray, D. C. & Leinwand, L. A. (1990) *J. Cell Biol.* **111**, 589–598.
10. Eghbali, B., Kessler, J. A. & Spray, D. C. (1990) *Proc. Natl. Acad. Sci. USA* **87**, 1328–1331.
11. Kunkel, T. A. (1985) *Proc. Natl. Acad. Sci., USA* **82**, 488–492.
12. Colby, W. W. & Shenk, T. (1982) *Proc. Natl. Acad. Sci. USA* **79**, 5189–5193.
13. Graham, F. L. & van der Eb, A. J. (1973) *Virology* **52**, 456.
14. Chen, C. A. & Okayama, H. (1989) *Biotechniques* **6**, 632–638.
15. Burt, J. M. & Spray, D. C. (1989) *Circ. Res.* **65**, 829–837.
16. Southern, P. J. & Berg, P. (1982) *J. Mol. Appl. Genet.* **1**, 327–341.
17. Berk, A. J. & Sharp, P. A. (1977) *Cell* **12**, 721–732.
18. Musil, L. S., Beyer, E. C. & Goodenough, D. A. (1990) *J. Membr. Biol.* **116**, 163–175.
19. Crow, D. S., Beyer, E. C., Paul, D. L., Kobe, S. S. & Lau, A. F. (1990) *Mol. Cell. Biol.* **10**, 1754–1763.
20. Neyton, J. & Trautmann, A. (1985) *Nature (London)* **317**, 331–335.
21. Spray, D. C., Saez, J. C., Brosius, D. A. & Bennett, M. V. L. (1986) *Proc. Natl. Acad. Sci. USA* **83**, 5494–5497.
22. Young, D. E., Cohn, Z. & Gilula, N. B. (1987) *Cell* **48**, 733–743.
23. Catterall, W. A. (1988) *Science* **242**, 50–61.
24. O'Dowd, B. F., Hantowich, M., Regan, J. W., Leader, W. M., Caron, J. G. & Lefkowitz, R. J. (1988) *J. Biol. Chem.* **263**, 15985–15992.
25. Stuhmer, W., Conti, F., Suzuki, H., Wang, X., Noda, M., Yahagi, N., Kubo, H. & Numa, S. (1989) *Nature (London)* **339**, 597–603.
26. Gorman, C. M., Merlino, G. T., Willingham, M. C., Pastan, I. & Howard, B. H. (1982) *Proc. Natl. Acad. Sci. USA* **79**, 6777–6781.